Title

Ziram, a pesticide associated with increased risk for Parkinson's disease, differentially affects the presynaptic function of aminergic and glutamatergic nerve terminals at the Drosophila neuromuscular junction

Journal

Experimental Neurology, 275(0 1)

ISSN

0014-4886

Authors

Martin, Ciara A
Myers, Katherine M
Chen, Audrey
et al.

Publication Date

2016

DOI

10.1016/j.expneurol.2015.09.017

Peer reviewed

Published in final edited form as:

Exp Neurol. 2016 January ; 275(0 1): 232–241. doi:10.1016/j.expneurol.2015.09.017.

Ziram, a pesticide associated with increased risk for Parkinson's disease, differentially affects the presynaptic function of aminergic and glutamatergic nerve terminals at the *Drosophila* neuromuscular junction

Ciara A. Martin[1,2,*], **Katherine M. Myers**[3,4,*], **Audrey Chen**[1,3,6], **Nathan T. Martin**[5], **Angel Barajas**[1], **Felix E. Schweizer**[3,4], and **David E. Krantz**[1,2,4]

Ciara A. Martin: martin.ciaraann@gmail.com; Katherine M. Myers: kmm2318@ucla.edu; Audrey Chen: audchen@caltech.edu; Nathan T. Martin: nathan.martin48@gmail.com; Angel Barajas: a.barajas40@gmail.com; Felix E. Schweizer: felixs@ucla.edu; David E. Krantz: dkrantz@ucla.edu

[1]Department of Psychiatry and Biobehavioral Sciences, Hatos Center For Neuropharmacology, David Geffen School of Medicine, University of California Los Angeles, Los Angeles, CA, 90095

[2]UCLA Interdepartmental Program in Molecular Toxicology, Los Angeles, CA 90095

[3]Department of Neurobiology, David Geffen School of Medicine, University of California Los Angeles, Los Angeles, CA, 90095

[4]UCLA Interdepartmental Program for Neuroscience, Los Angeles, CA 90095

[5]UCLA Biomedical Physics Interdepartmental Graduate Program, Los Angeles, CA, 90095

Abstract

Multiple populations of aminergic neurons are affected in Parkinson's disease (PD), with serotonergic and noradrenergic loci responsible for some non-motor symptoms. Environmental toxins, such as the dithiocarbamate fungicide ziram, significantly increase the risk of developing PD and the attendant spectrum of both motor and non-motor symptoms. The mechanisms by which ziram and other environmental toxins increase the risk of PD, and the potential effects of these toxins on aminergic neurons, remain unclear. To determine the relative effects of ziram on the synaptic function of aminergic versus non-aminergic neurons, we used live-imaging at the *Drosophila melanogaster* larval neuromuscular junction (NMJ). In contrast to nearly all other studies of this model synapse, we imaged presynaptic function at both glutamatergic Type Ib and aminergic Type II boutons, the latter responsible for storage and release of octopamine, the invertebrate equivalent of noradrenalin. To quantify the kinetics of exo- and endo- cytosis, we

Correspondence: David E. Krantz M.D., Ph.D., Gonda (Goldschmied) Neuroscience and Genetics Research Center, Room 3357C, 695. Charles E. Young Dr. South, David Geffen School of Medicine, University of California, Los Angeles, Los Angeles, CA 90095, (310) 206-8508, dkrantz@ucla.edu.
GLawless@mednet.ucla.edu
[6]Current address: Division of Biology and Biological Engineering, California Institute of Technology, Pasadena, CA 91125
*equal contribution

Financial interests declaration: None.

employed an acid-sensitive form of GFP fused to the *Drosophila* vesicular monoamine transporter (DVMAT-pHluorin). Additional genetic probes were used to visualize intracellular calcium flux (GCaMP) and voltage changes (ArcLight). We find that at glutamatergic Type Ib terminals, exposure to ziram increases exocytosis and inhibits endocytosis. By contrast, at octopaminergic Type II terminals, ziram has no detectable effect on exocytosis and dramatically inhibits endocytosis. In contrast to other reports on the neuronal effects of ziram, these effects do not appear to result from perturbation of the UPS or calcium homeostasis. Unexpectedly, ziram also caused spontaneous and synchronized bursts of calcium influx (measured by GCaMP) and electrical activity (measured by ArcLight) at aminergic Type II, but not glutamatergic Type Ib, nerve terminals. These events are sensitive to both tetrodotoxin and cadmium chloride, and thus appear to represent spontaneous depolarizations followed by calcium influx into Type II terminals. We speculate that the differential effects of ziram on Type II versus Type Ib terminals may be relevant to the specific sensitivity of aminergic neurons in PD, and suggest that changes neuronal excitability could contribute to the increased risk for PD caused by exposure to ziram. We also suggest that the fly NMJ will be useful to explore the synaptic effects of other pesticides associated with an increased risk of PD.

Keywords

ziram; dithiocarbamate; neuronal excitability; Parkinson's disease; *Drosophila*; dopamine; octopamine; pesticide; fungicide

Introduction

Parkinson's disease (PD) is a prevalent neurodegenerative disease best known for movement deficits and dopamine (DA) neuron loss in the substantia nigra (Corti et al., 2011). However, other populations of aminergic neurons are also affected in PD and are responsible for many non-motor symptoms of PD such as depression, insomnia and gastrointestinal dysfunction (Kuhn et al., 2011; Politis et al., 2012; Taylor et al., 2009). It remains unclear why aminergic neurons are particularly susceptible to the pathogenic mechanisms of PD, but several recent studies highlight the potential importance of alterations in neuronal excitability (Dragicevic et al., 2015).

While several heritable forms of PD have been identified, the vast majority of cases are sporadic, suggesting the possibility that environmental exposures play a role in disease etiology. Recent epidemiological data demonstrate that exposure to the fungicide ziram increases the risk of PD two-fold (Fitzmaurice et al., 2014; Rhodes et al., 2013; Wang et al., 2011). Risk is further increased to three-fold in individuals exposed to ziram in addition to the herbicide paraquat and the fungicide maneb (Wang et al., 2011). Ziram, maneb and paraquat can each selectively kill aminergic neurons *in vitro* and *in vivo* (Chou et al., 2008; Cicchetti et al., 2005; McCormack et al., 2002; Meco, 1994). It remains unclear why these environmental toxins show relatively selective neurotoxic effects in aminergic cells.

There are several proposed mechanisms by which ziram might exert its neurotoxic effects. Ziram directly inhibits the enzyme aldehyde dehydrogenase (ALDH) which is responsible for the detoxification of multiple oxidative species including dopamine metabolites

(Fitzmaurice, 2012). Ziram also directly inhibits E1 ligase (Chou et al., 2008; Rinetti and Schweizer, 2010), the first enzyme in the biochemical cascade responsible for protein ubiquitination (Ciechanover, 1994; Kleiger and Mayor, 2014). Although the precise protein targets are not known, ziram impairs mitochondrial function (Li et al., 2012; Yamano and Morita, 1995) depletes cellular sulfhydryls (Yamano and Morita, 1995) and disrupts calcium homeostasis in some cell types, possibly through effects on the Sodium Calcium Exchanger NCX3 or a non-specific cation channel (Jin et al., 2014b; Sook Han et al., 2003). More specifically neuronal effects of ziram include an increase in spontaneous synaptic events (miniature Excitatory Post-Synaptic Currents and Inhibitory Post-Synaptic Currents, mEPSCs and mIPSCs) recorded in postsynaptic hippocampal neurons, consistent with an increased probability of presynaptic vesicle fusion (Rinetti and Schweizer, 2010). Inhibition of E1 ligase activity by other drugs (MG1-32, lactacystin) also increases spontaneous vesicle fusion (Rinetti and Schweizer, 2010) but the mechanism remains incompletely understood. It is possible that ziram has additional synaptic effects relevant to either its neurotoxic potential and/or its ability to increase the risk for PD.

The disruption of presynaptic activity in hippocampal neurons prompted us to explore the presynaptic effects of ziram on another well-characterized model synapse, the *Drosophila* larval neuromuscular junction (NMJ) (Gramates and Budnik, 1999). Unlike mammals, which release acetylcholine as a fast-acting acting excitatory neurotransmitter at the NMJ, flies release glutamate, similar to excitatory synapses in the mammalian CNS. Glutamatergic synapses at the fly NMJ include Type Ib (big) and Is (small) (Atwood et al., 1993; Jan and Jan, 1976; Jia et al., 1993). Importantly, the larval NMJ contains two other types of synapses that are not glutamatergic: Type II terminals that store and release the aminergic neurotransmitter octopamine and Type III terminals that release peptide neurotransmitters (Atwood et al., 1993; Jia et al., 1993; Monastirioti et al., 1995). Since octopamine is structurally and functionally similar to mammalian noradrenaline (Roeder, 2004), Type II boutons provide a model for neurons that store and release amines other than dopamine that are sensitive to the pathophysiology of PD (Kuhn et al., 2011; Politis et al., 2012; Taylor et al., 2009).

Despite their potential use to model PD and synaptic function in general, relatively few studies of the fly NMJ have focused on Type II terminals because octopamine, like most mammalian amines, does not activate ionotropic receptors and cannot be followed via postsynaptic electrophysiological recordings. Other methods to quantify presynaptic function such as FM dyes or genetic probes can be used to study the activity of aminergic Type II terminals, but surprisingly, to our knowledge this has not yet been reported.

Here we have used genetic probes for vesicle recycling, voltage changes and calcium to compare the effects of ziram on aminergic Type II versus glutamatergic Type Ib nerve terminals. We report unexpected differences in their respective responses to toxin exposure including an increase in the spontaneous depolarization of aminergic, but not glutamatergic, processes. These differences may be relevant to the selective neurotoxic effects of ziram on mammalian aminergic neurons *in vitro* (Chou et al., 2008) and the observed increased risk for PD associated with ziram exposure in humans (Fitzmaurice et al., 2014; Rhodes et al., 2013; Wang et al., 2011).

Materials and Methods

Fly husbandry

Flies were reared on standard molasses yeast agar at room temperature. Flies expressing E1 RNAi and DVMAT-pHluorin were generated as described in (Martin et al., 2014) and (Grygoruk et al., 2014), respectively, and are available on request. Other lines including *elav-GAL4(X)* (Robinow and White, 1991), *Tdc2-GAL4* (Cole et al., 2005), *DVGLUT-GAL4* (Daniels et al., 2004), *UAS-Arclight* (Cao et al., 2013) and *UAS-GCaMP6m(III)* (Chen et al., 2013) are available from the Bloomington Stock Center. For pHluorin imaging experiments, *UAS-DVMAT-pHluorin(III) was expressed using elav-GAL4(X).* For pHluorin imaging experiments involving E1 RNAi, F_1 progeny were collected from *elav-GAL4;+;UAS-DVMAT-pHluorin* females crossed to *+;+;UAS-E1-RNAi* males. Controls for these experiments included F_1 progeny from e*lav-GAL4;+;UAS-DVMAT-pHluorin* females crossed to Canton S (wild type) males. F_1 progeny used for calcium imaging were derived from *elav-GAL4* females crossed to *UAS-GCaMP6m (III)* males. For experiments using *UAS-ArcLight*, F_1 progeny were derived from *DVGLUT-GAL4* or *Tdc2-GAL4* females crossed to *UAS-ArcLight* males.

pHluorin imaging

To visualize DVMAT-pHluorin, fillets of third instar larvae were prepared in chilled HL3.1 Ca^{2+}-free media (final mM concentration: NaCl 70, KCl 5, $MgCl_2$ 4, $NaHCO_3$ 10, trehalose 5, sucrose 115, HEPES 5) adjusted to pH 7.32 (Feng et al., 2004). Stock solutions of 10 mM ziram were made in Dimethyl Sulfoxide (DMSO, Sigma, St. Louis, MO), aliquoted, stored at −20°C and discarded after one freeze-thaw cycle; stocks of 10 mM lactacystin (Sigma, St. Louis, MO) were made in ddH_2O and treated as for ziram. Fresh stocks of L-glutamic acid (LGA) (Sigma, St. Louis, MO) were made weekly, and fresh stocks of HL3.1 were made monthly. LGA, $CaCl_2$, ziram, lactacystin or vehicle (DMSO) were added to HL3.1 on the day of the experiment. For ziram preincubation in Figures 1–3, fillets were incubated for 45 minutes at 18oC in ‘recording solution’ (HL3.1 supplemented with 2 mM calcium and 700 μM L-glutamic acid to suppress muscle contractions) and containing either 20 μM ziram (Chem Services, West Chester, PA) or DMSO as a control (final DMSO concentration 0.2%). After incubation, the fillets were washed 3x in chilled recording solution prior to imaging. Experiments involving lactacystin were conducted the same as the ziram preincubation experiments, but with the addition of 100 μM lactacystin or vehicle alone (ddH_2O) as indicated.

Nerve terminals were imaged using a Zeiss Axio Examiner Z1 microscope and Zeiss Achroplan water-immersion objective (100x, 1.0 N.A.) fitted with a cooled back-illuminated electron-multiplying CCD camera (Andor iXon 897, South Windsor, CT) and a capture rate of 20 frames/second using Andor IQ2 software. A DG4 light source (Sutter, Novato, CA) with a GFP Brightline® Filter Set (Semrock, Rochester, NY) was used for illumination. Segment A4 muscle 13 was visualized for all experiments. To stimulate exocytosis, a suction electrode was used to stimulate a single nerve root (10 V, 40 Hz for 2 seconds). Exocytosis was quantified as maximal $\Delta F/F = [(F_{peak} - F_{baseline})/F_{baseline}]*100$, where F_{peak} is the average fluorescence for the ten frames (0.5s) after the end of the 2 sec stimulus

period and $F_{baseline}$ is the average of the ten frames immediately preceding stimulus. We observed minimal decay in many of the endocytic curves for Type II terminals, prohibiting the calculation of tau by fitting a non-linear exponential curve. Therefore, to directly compare Type Ib and Type II terminals, we quantified endocytosis for all curves as the decrease in fluorescence due to endocytosis as % of F_{peak} at t = 10 sec post stimulus as described (Grygoruk et al., 2014).

Calcium imaging

To monitor intracellular calcium concentrations, a calcium sensitive form of GFP, *UAS-GCaMP6* (Chen et al., 2013) was expressed pan-neuronally using *elav-GAL4(X)* (Robinow and White, 1991). Larvae were dissected as for pHluorin experiments and either 1) preincubated in 20 μM ziram (0.2 % DMSO) or DMSO alone for 45 minutes (18°C) followed by washing in recording solution (Figure 4) or 2) imaged during continuous incubation in recording solution containing either 20 μM ziram (0.2 % DMSO) or DMSO alone at ambient temperature (Figure 5). For evoked response recordings, nerve roots were stimulated (10 V, 40 Hz for 2 seconds) and imaged as for DVMAT-pHluorin. Due to differences in the kinetics of the pH (pHluorin) versus calcium- sensitive (GCaMP) GFP-based probes, ΔF/F was calculated for GCaMP as $[(F_{peak} - F_{baseline})/F_{baseline}]*100$, with F_{peak} representing the average of four frames right before and four frames right after the end of stimulus (0.4 sec total) (Macleod, 2012) with $F_{baseline}$ representing the average of the ten frames prior to stimulus (0.5 seconds total).

For experiments involving the channel inhibitors tetrodotoxin (TTX) and Cadmium Chloride ($CdCl_2$), larval fillets were imaged in recording solution (HL3.1 with 2 mM calcium and 700 μM L-glutamic acid) plus 0.2% DMSO +/− 20 μM ziram without channel inhibitor, then washed 3x with recording solution containing either 20 μM ziram or 20 μM ziram plus 1 μM TTX or 100 μM $CdCl_2$. After incubation in this solution for an additional 5 minutes, the preparations were imaged for ≥ 1.2 minutes.

ArcLight Recordings

To monitor intracellular voltage changes, a voltage sensitive form of GFP, *UAS-ArcLight* was expressed in either octopaminergic neurons using the *Tdc2-GAL4* driver or glutamatergic using the *DVGLUT-GAL4* driver. Larvae were dissected as for pHluorin experiments and imaged during continuous incubation in recording solution containing either 20 μM ziram (0.2 % DMSO) or DMSO alone at ambient temperature. (Note that in Figure 6 the fluorescence signal from ArcLight decreases in response to depolarizations in contrast to the increase in fluorescence seen with GCaMP in Figures 5.)

Data Analysis

Averaged data in the figures are presented as mean ± SEM. The number of recordings (max 2 per fillet) was used as the statistical n throughout. For each recording, 1–7 boutons were imaged and averaged as a single n. Boutons that moved out of the z plane during or after a stimulus were not analyzed. Statistical analysis was carried out in Graphpad Prism. To avoid assumptions about the nature of the data (e.g. whether it was normally distributed) a non-parametric Mann-Whitney test was used throughout. An effect was judged statistically

significant if $p < 0.05$. A custom script written in the R programming language (Gnu Operating System) was used to quantify the average amplitude and frequency of some spontaneous events. An additional custom script in R was used to perform resampling statistical analysis ("bootstrapping") of the E1 RNAi data.

Results

Ziram exposure at glutamatergic terminals results in aberrant exo- and endocytosis

To further explore the presynaptic effects of ziram (Rinetti and Schweizer, 2010), we used the well-characterized neuromuscular junction (NMJ) of the *Drosophila* 3rd instar larva (Jan and Jan, 1976). Standard fillet preparations were used and the exposed abdominal musculature and NMJ was pre-incubated in ziram. To induce exocytosis, a nerve root innervating a selected muscle was stimulated (see Methods). We first recorded evoked DVMAT-pHluorin exo- and endocytosis at the canonical Type Ib excitatory nerve terminals (Figure 1A–D). Ziram exposure at Type Ib terminals caused a significant increase in exocytosis relative to preparations incubated in vehicle alone, with ΔF/F values of 21.9% ± 1.7 of baseline for control versus 30.6% ± 2.8 for ziram-treated preps (Mean ± SEM) (Figure 1C; n= 23–25 fillets per treatment; Mann-Whitney test, $p < 0.01$). We also observed a modest decrease in obligate endocytosis that occurs following cessation of the stimulus, with % of F_{peak} at t = 10 sec post stimulus 6.2% ± 5.6 for control versus 14.7% ± 7.5 for ziram-treated preps (Figure 1D; n = 23–25 fillets per treatment; Mann-Whitney test, $p < 0.01$). In sum, at glutamatergic, Type Ib terminals, ziram increases evoked exocytosis and modestly retards endocytosis.

Ziram exposure at aminergic terminals disrupts endocytosis but not exocytosis

To determine how ziram exposure might affect synaptic function at aminergic Type II terminals (Figure 2A–D), we again exposed larval fillets to ziram followed by stimulation of the nerve root in the absence of ziram and imaged as described for Type Ib terminals. Under control conditions, exocytosis was higher in Type II terminals compared to Type Ib with an average maximal ΔF/F of 53% versus 22% at Type Ib terminals (compare Figure 1C, 2C). However, in contrast to Type Ib terminals, exocytosis at Type II terminals exposed to ziram did not significantly differ from DMSO controls, with ΔF/F values of 52.9% ± 7.1 for control versus 59.1% ± 10.4 for treated preps (Figure 2C; n = 18–20 per treatment; Mann-Whitney test, $p > 0.05$). Endocytosis at Type II terminals was generally slower than Type Ib in control conditions, with the average return to baseline occurring at 17s versus 12s (compare Figures 1D, 2D). Endocytosis was further slowed at Type II terminals following exposure to ziram, with ziram-treated fillets showing a decay at t = 10 seconds post-stimulus to 37.5% ± 8.0 of peak versus 8.1% ± 11.7 in controls (Figure 2D; n = 18–20 per treatment; Mann-Whitney test, $p < 0.05$). In sum, Type II terminals exhibit a clear slowing of in endocytosis without a detectable change in exocytosis following ziram exposure, a pattern different from that observed in Type Ib terminals.

Inhibition of components of the Ubiquitin Proteasome System does not mimic ziram's effect at Type Ib or Type II terminals

Ziram inhibits the ubiquitin activating E1 ligase and inhibition of the Ubiquitin Proteasome System (UPS) may underlie some of the effects of ziram at mammalian nerve terminals (Chou et al., 2008; Rinetti and Schweizer, 2010). Exposure to proteasome inhibitors has also been suggested to increase the evoked response at the fly NMJ (Speese et al., 2003). By contrast, we did not observe any change in exocytosis using the proteasome inhibitor lactacystin (100 μm) at Type Ib terminals (Figure 3A; n = 18–21 per treatment; Mann-Whitney test, $p > 0.05$). Similarly, lactacystin exposure did not appear to affect endocytosis, as measured by % peak at 10s post-stimulus, at Type Ib terminals (Figure 3B; n = 18–21 per treatment, Mann-Whitney test, $p > 0.05$). A previously described degron transgene (Pandey et al., 2007) was used to confirm that UPS function was indeed disrupted by incubation in ziram (Supplemental Figure 1). Taken together, these data suggest that inhibition of the proteasome may not be responsible for the increase in exocytosis or the slight decrease in endocytosis we observe in ziram-treated Type Ib terminals.

To further evaluate the potential effects of ubiquitin E1 ligase inhibition, we used a genetic approach. RNAi representing *Drosophila* E1 ligase was expressed at Type Ib terminals (see Methods) and DVMAT-pHluorin was imaged as in Figures 1 and 2. As in our experiments using lactacystin, a degron transgene was used as a positive control to demonstrate the disruption of UPS function by E1 RNAi (Supplemental Figures 2 and 3). Metrics for exo- nor endo- cytosis did not significantly differ from controls (Figure 3C, D, n = 10–12; Mann-Whitney test, $p > 0.05$). We noted a trend toward a decreased maximum $\Delta F/F$ in lines expressing RNAi for E1 ligase (Mann-Whitney, $p = 0.08$). Using resampling statistics instead of a non-parametric approach yielded $p = 0.04$ for the difference of the medians. We conclude that there is a weak trend towards *decreased* exocytosis but note that the direction of this trend is the *opposite* of the effect seen in Type Ib terminals treated with ziram. It thus is highly unlikely that the ziram-induced *increase* in exocytosis at Type Ib terminals is due to an inhibition of E1 ligase activity.

We next tested the effects of E1 ligase RNAi and lactacystin at Type II terminals. Neither treatment altered exo- or endocytosis at Type II terminals (Figure 3E–H). The differences between the effects of ziram and those of either lactacystin or E1 RNAi suggest that ziram may influence the exocytotic cycle in Type Ib and II terminals via mechanisms that do not involve the UPS.

Ziram exposure does not alter baseline calcium levels or calcium influx during exocytosis at Type Ib or Type II terminals

Ziram exposure has been shown to increase levels of intracellular calcium in PC12 (Sook Han et al., 2003) and in BHK cells (Jin et al., 2014a) and calcium is tightly coupled with the release of secretory vesicles. We therefore examined whether the ziram-induced increase in exocytosis we observed in Type Ib terminals might be due to higher baseline calcium concentrations and/or an increase in calcium influx during stimulation. To address this question, we expressed the genetically encoded calcium indicator GCaMP6 and imaged the Type Ib (Figure 4A–C) and Type II boutons (Figure 4D–F) after exposure to ziram (20 μM

ziram for 45 minutes followed by recording in the absence of ziram). Exocytosis was initiated as for pHluorin imaging via electrical stimulation of a nerve root (10 V, 40 Hz for 2 seconds). Exposure to ziram did not result in a detectable increase in calcium influx during stimulus-evoked exocytosis at Type Ib boutons (Figure 4B; n=11 per treatment; Mann-Whitney test, $p > 0.05$), or detectably alter baseline calcium levels (Figure 4C; n = 11 per treatment; Mann-Whitney test, $p > 0.05$). These data suggest that neither an increase in calcium influx during exocytosis nor changes in baseline calcium levels are responsible for the increase in exocytosis we observe at ziram-treated Type Ib terminals.

For completeness, we similarly tested the potential effects of ziram exposure on calcium dynamics at Type II terminals. As expected, we did not detect a statistically significant difference in either baseline calcium levels or evoked calcium influx in ziram-exposed fillets versus controls (Figure 4D–G n = 7–21 per treatment; Mann-Whitney test, $p > 0.05$).

We note that the evoked calcium response for Type Ib and Type II terminals show a distinctly different time course under baseline conditions. Type II terminals exhibit an immediate increase in GCaMP fluorescence, followed by a plateau during stimulus and a gradual decay. By contrast, Type Ib terminals exhibit a more gradual increase in fluorescence that peaks near the end of stimulus and then immediately declines. These differences reinforce the notion that baseline synaptic function in Type Ib and Type II terminals is likely divergent, consistent with the differences we observe in their response to ziram.

Ziram exposure causes spontaneous calcium events in Type II aminergic, but not Type Ib glutamatergic, terminals

While conducting baseline and evoked calcium recordings following pre-incubation in ziram at 18°C, we observed spontaneous and synchronized spikes of GCaMP6 fluorescence in aminergic Type II terminals but not in Type Ib terminals. To explore this phenomenon, larval fillets expressing GCaMP6 pan-neuronally were incubated in 20 μM ziram at ambient temperature while continuously imaging the NMJ. Repetitive, spontaneous calcium events were observed in Type II terminals within 5–10 minutes of ziram exposure in all experiments (Figure 5B, n = 6, one representative trace is shown) but not following incubation in vehicle alone (not shown, n = 8). Spontaneous calcium events were never observed in Type Ib terminals or the slightly smaller and glutamatergic Type Is terminals (data not shown). Quantification of spontaneous calcium events in Type II terminals after 10 minutes of incubation in ziram indicated an average frequency of 8.0 ± 1.0 events/minute, with an average amplitude of 25.8 ± 5.6 $\Delta F/F$ (n = 6). We did not detect a change in either baseline calcium levels or in evoked calcium influx under these conditions (data not shown) consistent with the notion that global changes in calcium homeostasis are unlikely to be responsible for the transient events we observe. Importantly, cytosolic calcium is highly buffered, and actively transported into intracellular stores and the extracellular milieu (Brini et al., 2014; Gleichmann and Mattson, 2011; Matthews and Dietrich, 2015). Thus, an increase in calcium transients can occur in the absence of elevated cytosolic levels.

Ziram induced spontaneous calcium events are sensitive to TTX and $CdCl_2$

We hypothesized that the calcium spikes observed in the presence of ziram might result from depolarization and/or propagation of an action potential in the observed axon. Since neuronal depolarization most often requires activation of sodium channels, we tested the effects of the sodium channel inhibitor tetrodotoxin (TTX). Co-incubation of TTX with ziram (Figure 5D, n=3, a representative trace is shown) blocked the spontaneous calcium events observed at aminergic terminals incubated with ziram alone (Figure 5C).

The calcium transients we observed at Type II terminals could represent intracellular calcium release, e.g. from the endoplasmic reticulum or calcium influx from the extracellular milieu, most likely mediated by voltage gated calcium channels as seen in a variety of other neurons (Simms and Zamponi, 2014). To test the latter hypothesis, we applied a broad inhibitor of voltage gated calcium channels, $CdCl_2$, to larval fillets exposed to ziram. Similar to TTX, $CdCl_2$ co-application with ziram ablated the spontaneous calcium transients of Type II terminals (Figure 5E; n= 3). Together, the effects of TTX and CdCl2 suggest that the calcium spikes we observe at Type II terminals in response to ziram are likely due to depolarization of the axon followed by influx of Ca through voltage gated calcium channels.

Incubation with lactacystin did not induce any detectable calcium spikes in Type II (or Type I) terminals (data not shown). Furthermore, co-incubation with lactascystin did not affect the ability of ziram to induce calcium spikes in Type II terminals (data not shown). These observations suggest that ziram-induced calcium spikes occur independently of the UPS, similar to the effects of ziram on the exocytotic cycle at the fly NMJ.

Ziram induces spontaneous depolarization of aminergic, but not glutamatergic, terminals

To further confirm that the ziram-induced synchronized calcium transients we observed at Type II terminals were mediated by axon depolarization, we conducted recordings using the voltage sensitive fluorescent reagent ArcLight. *UAS-ArcLight* was expressed in Type II octopaminergic neurons of the NMJ using the *Tdc2-GAL4* driver or in Type Ib glutamatergic neurons using the *DVGLUT-GAL4* driver (Figure 6A,B). Recordings were taken at baseline (Figure 6A), and following 10 min of continuous 20 μM ziram incubation while simultaneously imaging the nerve terminals (Figure 6B). No events were observed in Type Ib glutamatergic terminals at baseline or after exposure to ziram (Figure 6A,B; n = 3). By contrast, spontaneous voltage driven events (average frequency 10.6 ± 1.4 events/minute) synchronized across all boutons, were consistently observed in Type II terminals to ziram (Figure 6D; n = 7) but not vehicle alone (data not shown). These data confirm that ziram induces spontaneous depolarizations in processes containing Type II terminals, consistent with an increase in excitability, but does not cause parallel excitatory changes in glutamatergic, Type Ib terminals.

Discussion

Epidemiological studies have demonstrated an increase in Parkinson's disease (PD) in human populations exposed to ziram and other pesticides (Fitzmaurice et al., 2014; Rhodes

et al., 2013; Wang et al., 2011), but the underlying mechanisms remain unclear. More fundamentally, the range of these pesticides effects on neurons and their influence on specific neuronal subtypes are not known. To investigate these questions, and more specifically explore the potential presynaptic effects of ziram, we have used the *Drosophila* neuromuscular junction (NMJ) as a model. To our knowledge, the fly NMJ has not been used previously to examine the effects of putative neurotoxins associated with PD. Importantly, our studies also differ from previous experiments using the fly NMJ because we have directly compared the synaptic physiology of two distinct types of nerve terminals: aminergic Type II and glutamatergic Type Ib terminals. We suggest that this comparison is relevant to the pathophysiology of PD since multiple subtypes of mammalian aminergic neurons are sensitive to the neurodegenerative processes that characterize this disease, including noradrenergic neurons of the locus coeruleus and serotonergic neurons in the raphe nuclei (Kuhn et al., 2011; Politis and Loane, 2011; Politis et al., 2012; Szot, 2012; Taylor et al., 2009). Using the fly NMJ, we observed striking differences in the effect of ziram on Type Ib glutamatergic versus Type II aminergic and suggest that these differences may be relevant to neurotoxic effects of ziram in mammals and perhaps PD patients. We anticipate that this system will be useful to explore the synaptic effects of other pesticides associated with an increased risk of PD.

In contrast to glutamatergic Type I terminals which have been extensively studied (Menon et al., 2013; Olsen and Keshishian, 2012), there is a striking paucity of data on the synaptic physiology of Type II aminergic terminals, in large part due to their lack of postsynaptic electrophysiological accessibility. We have circumvented this issue by taking advantage of genetically expressed fluorescent indicators of presynaptic activity. Using a *DVMAT-pHluorin* transgene and live-imaging techniques, we have shown that ziram treatment delays endocytosis in Type II and, to a lesser extent, Type Ib terminals. By contrast, we observe an increase in exocytosis in Type Ib, but no detectable change in exocytosis in Type II in response to ziram exposure. Using the additional transgenic probe GCaMP to image calcium dynamics, we did not detect an increase in baseline or evoked calcium levels suggesting that the disruption of exo- and endo-cytosis was not due to increased calcium influx. However, we observed a striking occurrence of spontaneous calcium transients in Type II, but not Type Ib, terminals. These events were blocked by tetrodotoxin and by $CdCl_2$, suggesting that ziram promotes spontaneous sodium-channel driven depolarizations that elicit calcium influx in Type II processes. We further confirmed this hypothesis using the voltage sensitive fluorescent transgene, ArcLight, and directly demonstrated spontaneous depolarizations in processes containing Type II, but not Type Ib, boutons. It remains unclear whether the effects of ziram on membrane trafficking and neuronal excitability are caused by the same or different underlying mechanisms, and further experiments will be needed to address this issue.

The increase in spontaneous depolarizations in Type II terminals demonstrates that ziram can cause an increase in excitability in a subset of aminergic neurons in the fly and perhaps other systems. These data are similar to the increase in aminergic excitability seen in several models of neurodegeneration and PD (Reviewed in (Dragicevic et al., 2015)). These include the increase in firing frequency of dopaminergic neurons over-expressing alpha-synuclein

(Subramaniam et al., 2014) or subjected to oxidative stress (Avshalumov et al., 2005). The effects of ziram-induced changes in exo- and endocytosis are more difficult to predict. However, an increase in evoked exocytosis seen in Type I terminals would be expected to cause an increase in glutamate release, and similar effects in the CNS could also lead to an increase in the excitation of downstream circuits. Future experiments to directly test these hypotheses and the effects of ziram exposure in fly as a whole may require parenteral administration; but it has proven difficult to administer neurotoxic doses of ziram through feeding (Martin et al., 2014).

It remains unclear how the proposed molecular targets of ziram could account for the effects on exocytosis and excitability that we observe. Ziram has been shown to inhibit E1 ligase, the enzyme responsible for ubiquitin activation prior to protein conjugation (Chou et al., 2008). Ubiquitin conjugation to proteins can result in a myriad of downstream effects in the neuron, including proteasomal degradation and regulation of endocytosis (DiAntonio and Hicke, 2004). Ziram-exposed primary hippocampal neurons exhibit an increase in mEPSPs that is mimicked by pharmacologic inhibition of ubiquitin E1 ligase (Rinetti and Schweizer, 2010). By contrast, we find that neither genetic inhibition of E1 ligase nor chemical inhibition of downstream proteasome activity induced spontaneous depolarizarion of Type II terminals or recapitulated the effect of ziram on exocytosis or endocytosis (as measured by pHluorin imaging). Also, in contrast to some other studies in mammalian cultured cells (Sook Han et al., 2003), we did not observe an effect of ziram on baseline calcium levels despite the occurrence of spontaneous calcium transients.

It remains possible that some of the effects of ziram at the fly NMJ result from disruption of mitochondrial activity (Yamano and Morita, 1995) or ALDH inhibition (Fitzmaurice et al., 2014). Alternatively, it is possible that other targets are responsible for the effects we observe (Stoytcheva, 2011). The activity of ziram as a thiol and its ability to deplete protein thiols in non-neuronal cells may be relevant to these effects (Shen, 2001). It interesting to note that other thiol-based toxins and the related drug disulfuram conjugate to a sulfur group in ALDH (Fitzmaurice et al., 2014; Shen, 2001, 2000) and the active site of E1 ligase also contains a critical cysteine residue (Ciechanover, 1994). We speculate that additional targets may be sensitive to the effects of ziram via conjugation to protein thiols and that these additional targets may be responsible for the effects of ziram we observe at the fly NMJ.

The spontaneous firing in Type II terminals seen with ziram exposure could result from a direct modification of channel activity. A number of mammalian channel subunits contain thiol groups that are sensitive to either nitrous oxide or exogenous thiol reagents (Ooi et al., 2013; Yang et al., 2013; Zhang and Horrigan, 2005). In addition, the dithiocarbamate pesticide mancozeb has been shown to activate the voltage-gated KCNQ2 potassium channel in CHO cells (Li et al., 2013). It is also possible that the relatively specific effects of ziram on Type II, but not Type Ib, terminals reflect the preferential activity of select channels in octopaminergic cells. Transcriptional analyses may help to identify channels potentially enriched in *Drosophila* aminergic neurons (Henry et al., 2012). In addition, electrophysiological studies in other insects have implicated several channels potentially involved in regulating the firing rates of octopaminergic neurons in *Drosophila* (Dugravot et

al., 2003; Gautier et al., 2008; Grolleau and Lapied, 2000; Heidel and Pflüger, 2006). One or more of these could be a target for ziram.

In mammals, a growing body of literature implicates altered channel activity in the pathogenesis of PD (Dragicevic et al., 2015). These include studies implicating the ATP gated potassium channels Kir6.2 in dopamine cell bursting and the neurodegenerative effects of MPTP (Liss et al., 2005; Schiemann et al., 2012), the oxidative effects of alpha-synuclein on A type potassium channels (Subramaniam et al., 2014), the loss of pacemaking activity in medium spiny neurons caused by disruption of a cyclic nucleotide-gated (HCN) potassium channel (Chan et al., 2011), and the contribution of calcium channels to mitochondrial dysfunction (Guzman et al., 2010). Investigating the contribution of these or other channels to our findings will be facilitated by the availability of mutations in most, if not all, channel genes in *Drosophila*. Although many of these mutations are lethal in the adult, nearly all survive as larvae, thus allowing a broad screen for mutations that mimic or block the effects of ziram.

At present, we cannot rule out the possibility that some of our data are idiosyncratic or specific to the larval NMJ, and further experiments using other neuronal subtypes in both flies and mammals are needed. We speculate, however, that the differences we observe between Type Ib and Type II boutons may represent a generalizable paradigm for the behavior of aminergic versus non-aminergic cells in response to ziram and perhaps other pesticides. If so, it is possible that the differential effects of ziram on Type Ib vs Type II are relevant to the sensitivity of aminergic pathways to the pathophysiologic processes that cause PD, and the effects of PD-related insults on neuronal excitability.

Supplementary Material

Refer to Web version on PubMed Central for supplementary material.

Acknowledgments

This work was conducted with funding from the National Institute of Environmental Health and Safety (NIEHS), UCLA training grant in Molecular Toxicology, USHHS Ruth L. Kirschstein Institutional National Research Service Award T32 ES015457, (C.A.M. pre-doctoral), NIEHS R01-ES015747 and NIMH R01-MH076900 (D.E.K.), NINDS R21-NS075506 (F.E.S), funding from the Parkinson's Disease Foundation (PDF-SFW-1336 to C.A.M.), from The Brain and Behavior Research Foundation and the Joanne and George Miller and Family Endowed Chair in Depression Research at the UCLA Brain Research Institute (D.E.K.), a pilot grant through the National Center for Advancing Translational Sciences UCLA CTSI Grant UL1TR000124 (F.E.S.) and an NIEHS program project grant ES016732 (M.F. Chesselet, PI).

Bibliography

Atwood HL, Govind CK, Wu CF. Differential ultrastructure of synaptic terminals on ventral longitudinal abdominal muscles in Drosophila larvae. Journal of Neurobiology. 1993; 24:1008–1024. [PubMed: 8409966]

Avshalumov MV, Chen BT, Koos T, Tepper JM, Rice ME. Endogenous hydrogen peroxide regulates the excitability of midbrain dopamine neurons via ATP-sensitive potassium channels. J Neurosci. 2005; 25:4222–4231. [PubMed: 15858048]

Brini M, Cali T, Ottolini D, Carafoli E. Neuronal calcium signaling: function and dysfunction. Cell Mol Life Sci. 2014; 71:2787–2814. [PubMed: 24442513]

Cao G, Platisa J, Pieribone VA, Raccuglia D, Kunst M, Nitabach MN. Genetically Targeted Optical Electrophysiology in Intact Neural Circuits. Cell. 2013; 154:10. doi:1016/j.cell.2013.1007.1027.

Chan CS, Glajch KE, Gertler TS, Guzman JN, Mercer JN, Lewis AS, Goldberg AB, Tkatch T, Shigemoto R, Fleming SM, et al. HCN channelopathy in external globus pallidus neurons in models of Parkinson's disease. Nat Neurosci. 2011; 14:85092.

Chen TW, Wardill T, Sun Y, Pulver SR, Renninger SL, Baohan A, Schreiter E, Kerr RA, Orger MB, Jayaraman V, et al. Ultrasensitive fluorescent proteins for imaging neuronal activity. Nature. 2013; 499:295–300. [PubMed: 23868258]

Chou AP, Maidment N, Klintenberg R, Casida JE, Li S, Fitzmaurice AG, Fernagut PO, Mortazavi F, Chesselet MF, Bronstein JM. Ziram Causes Dopaminergic Cell Damage by Inhibiting E1 Ligase of the Proteasome. Journal of Biological Chemistry. 2008; 283:34696–34703. [PubMed: 18818210]

Cicchetti F, Lapointe N, Roberge-Tremblay A, Saint-Pierre M, Jimenez L, Ficke BW, Gross RE. Systemic exposure to paraquat and maneb models early Parkinson's disease in young adult rats. Neurobiol Dis. 2005; 20:360–371. [PubMed: 16242641]

Ciechanover A. The ubiquitin-proteasome proteolytic pathway. Cell. 1994; 79:13–21. [PubMed: 7923371]

Cole SH, Carney GE, McClung CA, Willard SS, Taylor BJ, Hirsh J. Two Functional but Noncomplementing Drosophila Tyrosine Decarboxylase Genes: Distinct role for neuronal tyramine and octopamine in female fertility. J Biol Chem. 2005; 280:14948–14955. [PubMed: 15691831]

Corti O, Lesage S, Brice A. What Genetics Tells us About the Causes and Mechanisms of Parkinson's Disease. Physiol Rev. 2011; 91:1161–1218. [PubMed: 22013209]

Daniels RW, Collins CA, Gelfand MV, Dant J, Brooks ES, Krantz DE, DiAntonio A. Increased expression of the Drosophila vesicular glutamate transporter leads to excess glutamate release and a compensatory decrease in quantal content. J Neurosci. 2004; 24:10466–10474. [PubMed: 15548661]

DiAntonio A, Hicke L. Ubiquitin-dependent regulation of the synapse. Annual Review of Neuroscience. 2004; 27:223–246.

Dragicevic E, Schiemann J, Liss B. Dopamine midbrain neurons in health and Parkinson's disease: Emerging roles of voltage-gated calcium channels and ATP-sensitive potassium channels. Neuroscience. 2015; 284:798–814. [PubMed: 25450964]

Dugravot S, Grolleau F, Macherel D, Rochetaing A, Hue B, Stankiewicz M, Huignard J, Lapied B. Dimethyl disulfide exerts insecticidal neurotoxicity through mitochondrial dysfunction and activation of insect K_ATP channels. Journal of Neurophysiology. 2003; 90:259–270. [PubMed: 12843310]

Feng Y, Ueda A, Wu CF. A MODIFIED MINIMAL HEMOLYMPH-LIKE SOLUTION, HL3.1, FOR PHYSIOLOGICAL RECORDINGS AT THE NEUROMUSCULAR JUNCTIONS OF NORMAL AND MUTANT DROSOPHILA LARVAE. Journal of Neurogenetics. 2004; 18:377–402. [PubMed: 15763995]

Fitzmaurice, AG. Dissertation, In Engineering and Applied Aciences. California Institute of Technology; 2012. The role of pesticide-induced aldehyde dehydrogenase inhibition in the pathogenesis of Parkinson's disease.

Fitzmaurice AG, Rhodes SL, Cockburn M, Ritz B, Bronstein JM. Aldehyde dehydrogenase variation enhances effect of pesticides associated with Parkinson disease. Neurology. 2014; 82:419–426. [PubMed: 24491970]

Gautier H, Auger J, Legros C, Lapied B. Calcium-activated potassium channels in insect pacemaker neurons as unexpected target site for the novel fumigant dimethyl disulfide. J Pharmacol Exp Ther. 2008; 324:149–159. [PubMed: 17942746]

Gleichmann M, Mattson MP. Neuronal calcium homeostasis and dysregulation. Antioxid Redox Signal. 2011; 14:1261–1273. [PubMed: 20626318]

Gramates, LS.; Budnik, V. Assembly and Maturation of the Drosophila Larval Neuromuscular Junction. In: Ronald, RAH.; Bradley, J.; Peter, J., editors. Int Rev Neurobiol. Academic Press; 1999. p. 93-117.

Grolleau F, Lapied B. Dorsal unpaired median neurones in the insect central nervous system: towards a better understanding of the ionic mechanisms underlying spontaneous electrical activity. The Journal of Experimental Biology. 2000

Grygoruk A, Chen A, Martin CA, Lawal HO, Fei H, Gutierrez G, Biedermann T, Najibi R, Hadi R, Chouhan AK, et al. The redistribution of Drosophila vesicular monoamine transporter mutants from synaptic vesicles to large dense-core vesicles impairs amine-dependent behaviors. J Neurosci. 2014; 34:6924–6937. [PubMed: 24828646]

Guzman JN, Sanchez-Padilla J, Wokosin D, Kondapalli J, Ilijic E, Schumacker PT, Surmeier DJ. Oxidant stress evoked by pacemaking in dopaminergic neurons is attenuated by DJ-1. Nature. 2010; 468:696–700. [PubMed: 21068725]

Heidel E, Pflüger HJ. Ion currents and spiking properties of identified subtypes of locust octopaminergic dorsal unpaired median neurons. Eur J Neurosci. 2006; 23:1189–1206. [PubMed: 16553782]

Henry GL, Davis FP, Picard S, Eddy SR. Cell type–specific genomics of Drosophila neurons. Nucleic Acids Res. 2012; 40:9691–9704. [PubMed: 22855560]

Jan LY, Jan YN. L-glutamate as an excitatory transmitter at the Drosophila larval neuromuscular junction. The Journal of Physiology. 1976; 262:215–236. [PubMed: 186587]

Jia XX, Gorczyca M, Budnik V. Ultrastructure of neuromuscular junctions in Drosophilal: Comparison of wild type and mutants with increased excitability. Journal of Neurobiology. 1993; 24:1025–1044. [PubMed: 8409967]

Jin J, Lao AJ, Katsura M, Caputo A, Schweizer FE, Sokolow S. Involvement of the sodium-calcium exchanger 3 (NCX3) in ziram-induced calcium dysregulation and toxicity. Neurotoxicology. 2014a

Jin J, Lao AJ, Katsura M, Caputo A, Schweizer FE, Sokolow S. Involvement of the sodium–calcium exchanger 3 (NCX3) in ziram-induced calcium dysregulation and toxicity. Neurotoxicology. 2014b; 45:56–66. [PubMed: 25284465]

Kleiger G, Mayor T. Perilous journey: a tour of the ubiquitin–proteasome system. Trends in Cell Biology. 2014

Kuhn DM, Sykes CE, Geddes TJ, Jaunarajs KLE, Bishop C. Tryptophan hydroxylase 2 aggregates through disulfide cross-linking upon oxidation: possible link to serotonin deficits and non-motor symptoms in Parkinson's disease. J Neurochem. 2011; 116:426–437. [PubMed: 21105877]

Li P, Zhu J, Kong Q, Jiang B, Wan X, Yue J, Li M, Jiang H, Li J, Gao Z. The ethylene bis-dithiocarbamate fungicide Mancozeb activates voltage-gated KCNQ2 potassium channel. Toxicol Lett. 2013; 219:211–217. [PubMed: 23542819]

Li Q, Kobayashi M, Kawada T. Mechanism of ziram-induced apoptosis in human T lymphocytes. Arch Toxicol. 2012; 86:615–623. [PubMed: 22159898]

Liss B, Haeckel O, Wildmann J, Miki T, Seino S, Roeper J. K-ATP channels promote the differential degeneration of dopaminergic midbrain neurons. Nat Neurosci. 2005; 8:1742–1751. [PubMed: 16299504]

Macleod GT. Calcium Imaging at the Drosophila Larval Neuromuscular Junction. Cold Spring Harb Protoc. 2012; 2012 pdb.top070078.

Martin CA, Barajas A, Lawless G, Lawal HO, Assani K, Lumintang YP, Nunez V, Krantz DE. Synergistic effects on dopamine cell death in a Drosophila model of chronic toxin exposure. Neurotoxicology. 2014

Matthews EA, Dietrich D. Buffer mobility and the regulation of neuronal calcium domains. Front Cell Neurosci. 2015; 9:48. [PubMed: 25750615]

McCormack AL, Thiruchelvam M, Manning-Bog AB, Thiffault C, Langston JW, Cory-Slechta DA, Di Monte DA. Environmental Risk Factors and Parkinson's Disease: Selective Degeneration of Nigral Dopaminergic Neurons Caused by the Herbicide Paraquat. Neurobiol Dis. 2002; 10:119–127. [PubMed: 12127150]

Meco G, Bonifati V, Vanacore N, Fabrizio E. Parkinsonism after chronic exposure to the fungicide maneb (manganese ethylene-bis-dithiocarbamate). Scand J Work Environ Health. 1994; 20:301–305. [PubMed: 7801076]

Menon KP, Carrillo RA, Zinn K. Development and plasticity of the Drosophila larval neuromuscular junction. Wiley interdisciplinary reviews Developmental biology. 2013; 2:647–670. [PubMed: 24014452]

Monastirioti M, Gorczyca M, Rapus J, Eckert M, White K, Budnik V. Octopamine immunoreactivity in the fruit fly Drosophila melanogaster. J Comp Neurol. 1995; 356:275–287. [PubMed: 7629319]

Olsen DP, Keshishian H. Experimental Methods for Examining Synaptic Plasticity in Drosophila. Cold Spring Harb Protoc. 2012; 2012 pdb.top067785.

Ooi L, Gigout S, Pettinger L, Gamper N. Triple cysteine module within M-type K+ channels mediates reciprocal channel modulation by nitric oxide and reactive oxygen species. J Neurosci. 2013; 33:6041–6046. [PubMed: 23554485]

Pandey UB, Nie Z, Batlevi Y, McCray BA, Ritson GP, Nedelsky NB, Schwartz SL, DiProspero NA, Knight MA, Schuldiner O, et al. HDAC6 rescues neurodegeneration and provides an essential link between autophagy and the UPS. Nature. 2007; 447:859–863. [PubMed: 17568747]

Politis M, Loane C. Serotonergic Dysfunction in Parkinson's Disease and Its Relevance to Disability. The Scientific World Journal. 2011; 11:9.

Politis M, Wu K, Loane C, Quinn NP, Brooks DJ, Oertel WH, Björklund A, Lindvall O, Piccini P. Serotonin Neuron Loss and Nonmotor Symptoms Continue in Parkinson's Patients Treated with Dopamine Grafts. Sci Transl Med. 2012; 4:128ra141.

Rhodes SL, Fitzmaurice AG, Cockburn M, Bronstein JM, Sinsheimer JS, Ritz B. Pesticides that inhibit the ubiquitin-proteasome system: effect measure modification by genetic variation in SKP1 in Parkinsons disease. Environ Res. 2013; 126:1–8. [PubMed: 23988235]

Rinetti GV, Schweizer FE. Ubiquitination Acutely Regulates Presynaptic Neurotransmitter Release in Mammalian Neurons. The Journal of Neuroscience. 2010; 30:3157–3166. [PubMed: 20203175]

Robinow S, White K. Characterization and spatial distribution of the ELAV protein during Drosophila melanogaster development. Journal of Neurobiology. 1991; 22:443–461. [PubMed: 1716300]

Roeder T. TYRAMINE AND OCTOPAMINE: Ruling Behavior and Metabolism. Annu Rev Entomol. 2004; 50:447–477. [PubMed: 15355245]

Schiemann J, Schlaudraff F, Klose V, Bingmer M, Seino S, Magill PJ, Zaghloul KA, Schneider G, Liss B, Roeper J. K-ATP channels in dopamine substantia nigra neurons control bursting and novelty-induced exploration. Nat Neurosci. 2012; 15:1272–1280. [PubMed: 22902720]

Shen M, Benson L, Johnson K, Lipsky J, Naylor S. Effect of Enzyme Inhibitors on Protein Quaternary Structure Determined by On-line Size Exclusion Chromatography-Microelectrospray Ionization Mass Spectrometry. J Am Soc Mass Spectrom. 2001; 12:97–104. [PubMed: 11142365]

Shen M, Lipsky J, Naylor S. Role of disulfiram in the in vitro inhibition of rat liver mitochondrial aldehyde dehydrogenase. Biochem Pharmacol. 2000; 60:947–953. [PubMed: 10974203]

Simms, Brett A.; Zamponi, Gerald W. Neuronal Voltage-Gated Calcium Channels: Structure, Function, and Dysfunction. Neuron. 2014; 82:24–45. [PubMed: 24698266]

Sook Han M, Shin KJ, Kim YH, Kim SH, Lee T, Kim E, Ho Ryu S, Suh PG. Thiram and Ziram Stimulate Non-Selective Cation Channel and Induce Apoptosis in PC12 Cells. Neurotoxicology. 2003; 24:425–434. [PubMed: 12782107]

Speese SD, Trotta N, Rodesch CK, Aravamudan B, Broadie K. The Ubiquitin Proteasome System Acutely Regulates Presynaptic Protein Turnover and Synaptic Efficacy. Current biology. 2003; 13:899–910. [PubMed: 12781128]

Stoytcheva, M. Pesticides in the Modern World - Effects of Pesticides Exposure. Rijeka, Croatia: InTech; 2011.

Subramaniam M, Althof D, Gispert S, Schwenk J, Auburger G, Kulik A, Fakler B, Roeper J. Mutant alpha-synuclein enhances firing frequencies in dopamine substantia nigra neurons by oxidative impairment of A-type potassium channels. J Neurosci. 2014; 34:13586–13599. [PubMed: 25297088]

Szot P. Common factors among Alzheimer's disease, Parkinson's disease, and epilepsy: Possible role of the noradrenergic nervous system. Epilepsia. 2012; 53:61–66. [PubMed: 22612810]

Taylor TN, Caudle WM, Shepherd KR, Noorian A, Jackson CR, Iuvone PM, Weinshenker D, Greene JG, Miller GW. Nonmotor symptoms of Parkinson's disease revealed in an animal model with reduced monoamine storage capacity. J Neurosci. 2009; 29:8103–8113. [PubMed: 19553450]

Wang A, Costello S, Cockburn M, Zhang X, Bronstein J, Ritz B. Parkinson's disease risk from ambient exposure to pesticides. Eur J Epidemiol. 2011; 26:547–555. [PubMed: 21505849]

Yamano T, Morita S. Effects of pesticides on isolated rat hepatocytes, mitochondria, and microsomes II. Arch Environ Contam Toxicol. 1995; 28:1–7. [PubMed: 7717759]

Yang Y, Jin X, Jiang C. S-Glutathionylation of Ion Channels: Insights into the Regulation of Channel Functions, Thiol Modification Crosstalk, and Mechanosensing. Antioxidants & Redox Signaling. 2013; 20:937–951. [PubMed: 23834398]

Zhang G, Horrigan FT. Cysteine Modification Alters Voltage- and Ca2+-dependent Gating of Large Conductance (BK) Potassium Channels. The Journal of General Physiology. 2005; 125:213–236. [PubMed: 15684095]

Highlights

- The dithiocarbamate fungicide ziram increases the risk for Parkinson's disease.
- The fly neuromuscular junction (NMJ) contains aminergic and glutamatergic terminals.
- Ziram differentially affects aminergic versus glutamatergic terminals at the fly NMJ.
- Ziram may increase the excitability of aminergic neurons.

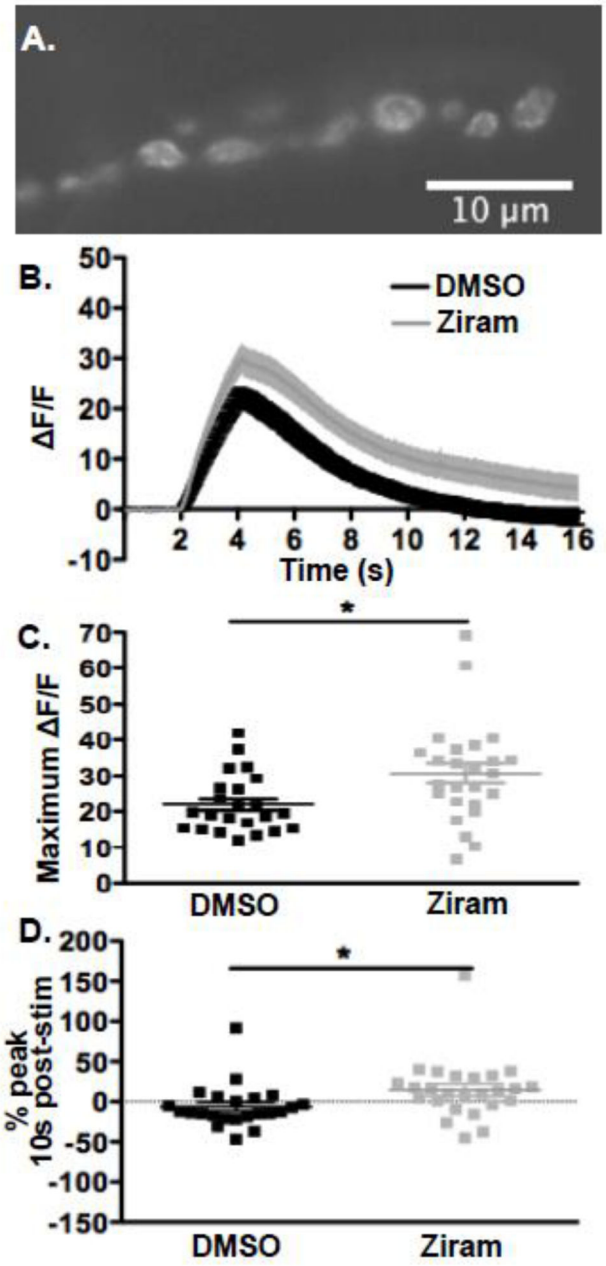

Figure 1. Exposure to ziram at excitatory glutamatergic terminals results in aberrant exo- and endo-cytosis

A) Representative image of baseline DVMAT-pHluorin signal at Type Ib boutons. Scale bar: 10 microns. B) Averaged trace (mean+/−SEM, n = 23–25 fillets) of Type Ib boutons exposed to ziram (20 µM, 45 min, light grey trace) or vehicle (dark grey), washed, and electrically stimulated (40 Hz, 2 sec) to induce exocytosis. C) Maximum ΔF/F was determined for control and ziram-treated preparations as a measure of exocytosis (Mann-Whitney test; n = 23–25 represented by each symbol; $p < 0.01$; mean+/−SEM also shown). D) To compare endocytic rates, the % peak fluorescence 10 seconds after stimulus was determined (Mann-Whitney test; n = 23–25; $p < 0.01$).

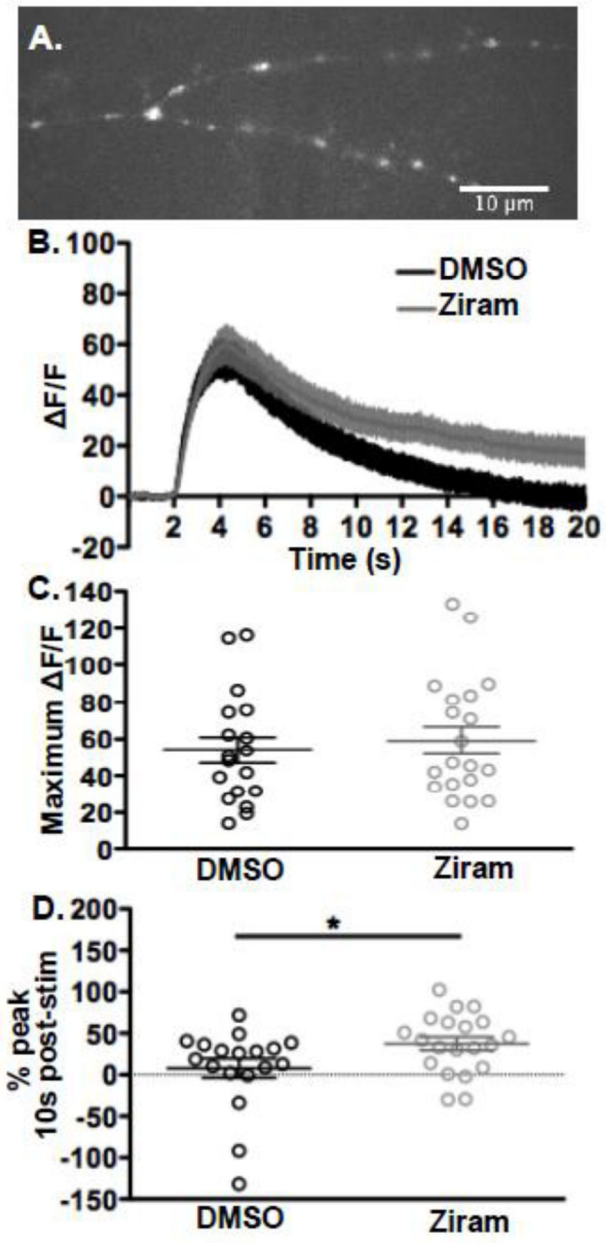

Figure 2. Exposure to ziram at aminergic terminals results in aberrant endocytosis

A) Representative image of baseline DVMAT-pHluorin signal in Type II boutons. Scale bar= 10 microns. B) Averaged traces from Type II boutons exposed to ziram (20 µM, 45 min, light grey trace) or vehicle (dark grey), washed, and electrically stimulated (40 Hz, 2 sec) to induce exocytosis. C) Maximum ΔF/F did not differ between Type II boutons treated with ziram versus vehicle alone (n = 18–20; Mann-Whitney test; $p > 0.05$). D) The % peak fluorescence at 10 seconds post stimulus was significantly higher in Type II boutons (n = 18–20; Mann-Whitney test; $p < 0.05$) suggesting a slower rate of endocytosis.

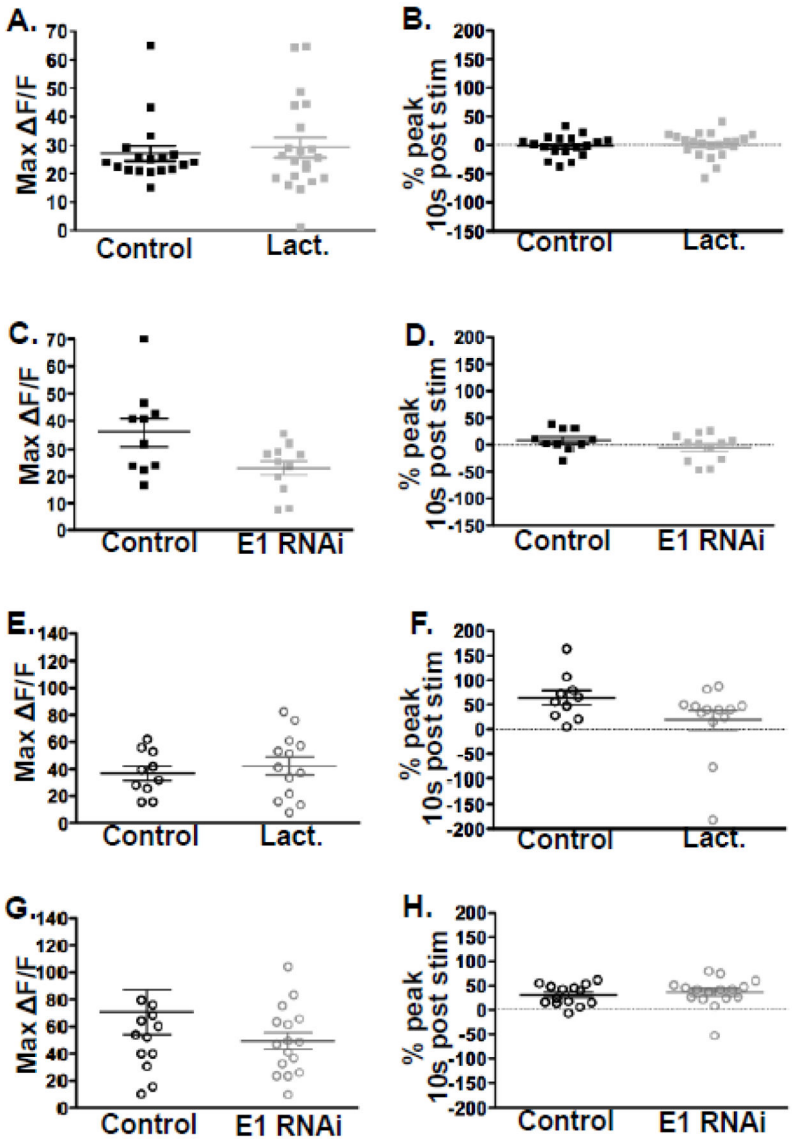

Figure 3. Inhibition of the Ubiquitin Proteasome System does not mimic ziram's action at the fly NMJ

A–B) Type Ib terminals were exposed to lactacystin (100 μM, 45 min) or vehicle, washed and imaged before and after stimulation (40 Hz, 2 sec). Neither the maximum ΔF/F (A) nor the % peak fluorescence at 10 seconds (B) differed between terminals exposed to lactacystin (light grey) versus vehicle alone (dark grey) (n = 18–21 per treatment, Mann-Whitney test, $p > 0.05$). C–D) Type Ib terminals expressing E1 RNAi (light grey) versus controls (dark grey). C) Maximum ΔF/F in Type Ib boutons expressing E1 RNAi (light grey) and the % of peak fluorescence at 10 seconds post stimulus (D) did not significantly differ (n = 10–12 per treatment, Mann-Whitney test, $p > 0.05$). E–H) Type II terminals exposed to lactacystin or expressing E1 RNAi were treated and analyzed identically to Type Ib terminals. Neither Maximum ΔF/F (E,G) nor % peak fluorescence 10 seconds post stimulus (F,H) differed significantly in Type II boutons treated with lactacystin (E, F, n = 10–13 per treatment,

Mann-Whitney test, $p > 0.05$) or expressing E1 RNAi (G, H; n = 14–16 per treatment, Mann-Whitney test, $p > 0.05$).

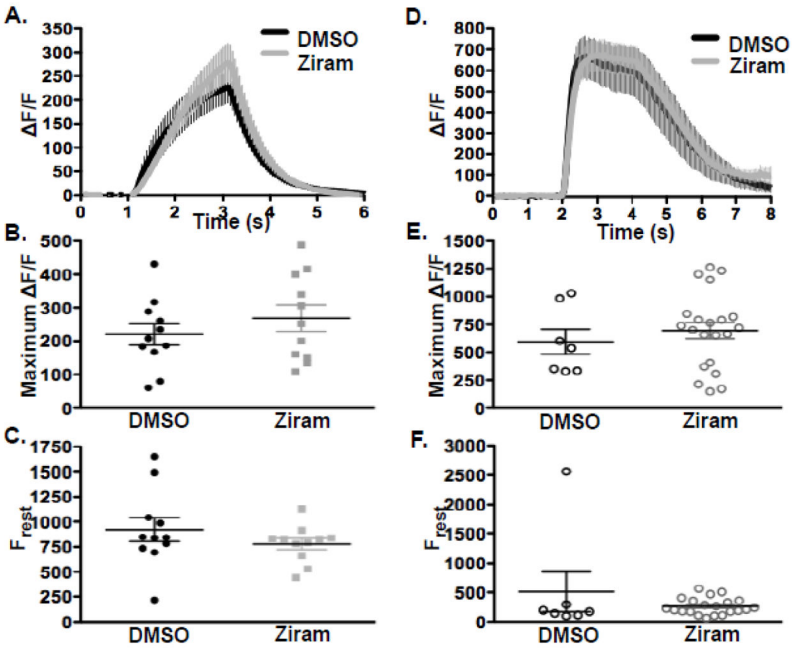

Figure 4. Ziram exposure does not alter calcium influx or baseline calcium levels at Type Ib or Type II synapses

Type Ib (A–C, n = 11 per treatment) or Type II boutons (D–F, n = 7–21 per treatment) expressing GCaMP were exposed to ziram (light grey, 100 μM, 45 min) or vehicle alone (DMSO, dark grey), washed and stimulated to induce calcium influx (40 Hz, 2 sec). Neither maximum ΔF/F (B, E) nor baseline fluorescence (C, F) showed statistically significant differences between preparations treated with ziram versus vehicle alone (Mann-Whitney test, $p > 0.05$).

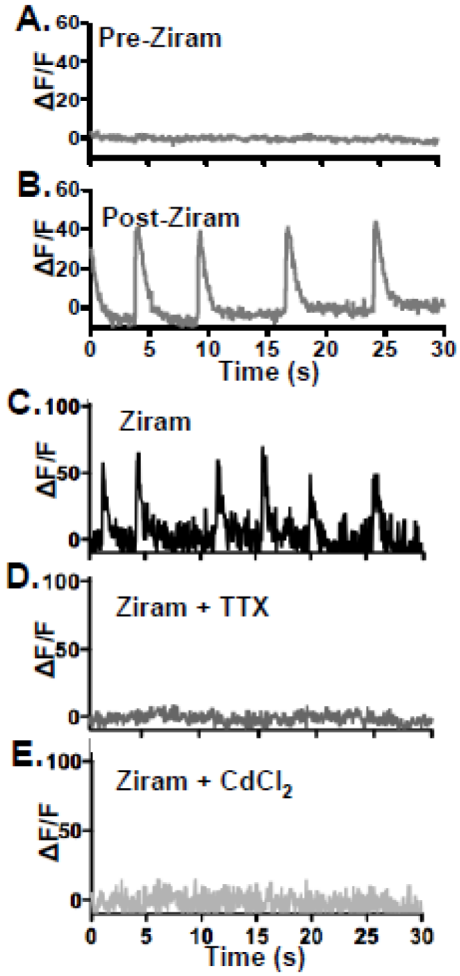

Figure 5. Ziram exposure causes coordinated and spontaneous calcium events in aminergic terminals

GCaMP fluorescence was quantified in Type II terminals exposed to vehicle (DMSO) alone (not shown) or 20μM ziram (A, B). Traces show repetitive calcium spikes after 10 minutes exposure to ziram (B, n = 6) but not at the onset of exposure (A) or in the presence of vehicle either at the onset of treatment or after 10 minute exposure (n = 8). C–D) Tetrodotoxin and $CdCl_2$ block ziram-induced spontaneous calcium events at aminergic terminals. Representative traces of Type II terminal from larval fillets treated with ziram (C, 20 μM, 10 min) followed by 5 min incubation in the same concentration of ziram plus either 1μM tetrodotoxin (D, n = 3) or 100 μM $CdCl_2$ (E, n = 3) to inhibit sodium and calcium channels respectively.

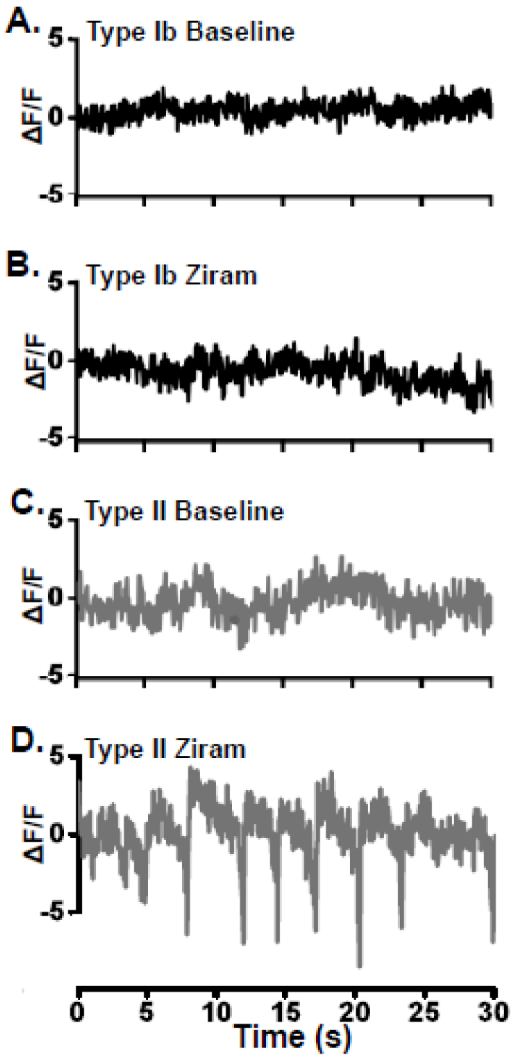

Figure 6. Ziram induces spontaneous voltage mediated events at aminergic terminals

Representative traces ArcLight recordings at a Type Ib terminal (A,B, n = 3 per treatment) and Type II terminal (C,D, n = 7 per treatment) before (A,C) and after (B,D) 10 min treatment with 20 μM ziram.